CONFIDENTIAL

Copy 1
RM E54D08

NACA RM E54D08

NACA

RESEARCH MEMORANDUM

ALTITUDE INVESTIGATION OF CAN-TYPE FLAME HOLDER IN 20-INCH-DIAMETER RAM-JET COMBUSTOR

By George R. Smolak and Carl B. Wentworth

Lewis Flight Propulsion Laboratory
Cleveland, Ohio

CLASSIFIED DOCUMENT

This material contains information affecting the National Defense of the United States within the meaning of the espionage laws, Title 18, U.S.C., Secs. 793 and 794, the transmission or revelation of which in any manner to an unauthorized person is prohibited by law.

NATIONAL ADVISORY COMMITTEE
FOR AERONAUTICS

WASHINGTON
June 3, 1954

CONFIDENTIAL

NATIONAL ADVISORY COMMITTEE FOR AERONAUTICS

RESEARCH MEMORANDUM

ALTITUDE INVESTIGATION OF CAN-TYPE FLAME HOLDER IN 20-INCH-DIAMETER RAM-JET COMBUSTOR

By George R. Smolak and Carl B. Wentworth

SUMMARY

An investigation of a can-type flame holder employing a fuel-air-mixture control sleeve in a 20-inch-diameter ram-jet combustor was conducted by free-jet and direct-connect techniques at a simulated flight Mach number of 3.0 and altitudes from about 70,000 to 80,000 feet.

The can-type combustor had peak combustor efficiencies of about 0.90 at fuel-air ratios of 0.018 and 0.04. The lower combustor efficiencies between these two fuel-air ratios were further reduced by reducing combustor-inlet pressure. Comparison with a previously reported circular V-gutter configuration revealed only slight differences in specific fuel consumption.

Reduction of the 86-inch combustion-chamber length to 56 inches lowered the combustor efficiency 14 percentage points at a fuel-air ratio of 0.02 and 18 percentage points at a fuel-air ratio of 0.04.

INTRODUCTION

As part of a program being conducted at the NACA Lewis laboratory to devise ram-jet combustors suitable for long-range missiles, the performance of a can-type flame holder has been investigated. The can-type flame holder is one of four flame holders which have been studied in the program. Results of tests on the other three flame holders, which included circular-gutter configurations with both small and large pilots and a sloping-baffle configuration with a large pilot, are reported in references 1 and 2. A direct-connect investigation of a 16-inch can-type flame holder at combustion-chamber inlet pressures of about 2400 pounds per square foot is reported in reference 3 and shows that high combustor efficiencies can be obtained over a wide range of fuel-air ratio (about 0.01 to 0.06) by use of a mixture control sleeve and dual fuel systems. It was the purpose of the investigation reported herein to extend the

investigation of reference 3 to combustor-inlet pressures below 2400 pounds per square foot. A similar can-type combustor was therefore investigated in a 20-inch-diameter ram-jet engine in an altitude chamber simulating a flight Mach number of 3.0.

The combustor efficiency, combustor total-pressure ratio, combustor-outlet total pressure, combustor-inlet Mach number, and specific fuel consumption are presented. The effect of combustor length on efficiency and the effect of pilot operating conditions on combustor burning limits are also presented.

APPARATUS

Facility

The facility that was utilized for this investigation could be operated as a free-jet and as a direct-connect unit. It is shown in figure 1 with the ram-jet combustor installed. Air entered the facility through a combustion-type preheater which vitiated the facility air supply to a fuel-air ratio of 0.009 or less. The air then passed into a surge tank and was expanded through a convergent-divergent nozzle to a Mach number of 3.0. The engine diffuser inlet was submerged in the Mach number 3.0 jet and the excess air spilled around the engine inlet through the jet diffuser. The engine exhaust passed into a separate chamber which could be throttled for engine starts. A complete description of the free-jet facility and its operation are given in reference 4.

For the direct-connect mode of investigation, blank-off plates were installed to cover the jet diffuser (fig. 1), so that air was ducted subsonically to the annulus formed by the engine cowl lip and the diffuser centerbody.

Engine

A cross section of the 20-inch-diameter, 173-inch-long ram-jet engine is shown in figure 2. The inlet diffuser is of the double-cone annular type with two external conical shocks. Axial centerbody support struts extending from near the cowl lip to about station 2 divide the air flow through the diffuser into three channels. The combustion chamber has an inside diameter of 20 inches and is water-jacketed. The contoured convergent exhaust nozzle has a minimum area equal to 55 percent of the combustion-chamber cross-sectional area.

A 6.4-inch-diameter, 4.9-inch-long pilot burner was mounted on the blunt end of the diffuser centerbody as shown in figure 2. Air was supplied to the pilot by three equally spaced nozzles designed to produce

whirling flow. Air was supplied to the pilot at the same temperature as the engine inlet air by bleeding it from the preheater discharge as shown in figure 1. Pilot fuel flow was introduced through a fixed-area conical spray nozzle located in the center of the upstream end of the pilot. The nozzle was rated at 12 gallons per hour at a differential pressure of 100 pounds per square inch.

A high-energy condenser-discharge ignition system was used to ignite the ram-jet engine. As shown in figure 2, the spark plug projected through the fuel-air mixture control sleeve and into the pilot burner.

The fuel used in the combustion preheater and the ram-jet engine was MIL-F-5624A, grade JP-4.

Combustor Configurations

Configuration 1. - Details of the can-type flame holder are shown in figure 2. The included cone angle of the can-type flame holder was 16.5°, and the ratio of surface open area of the can-type flame holder to combustion-chamber cross-sectional area was 1.17. These design variables were nearly the same as those used for the can-type flame holder of reference 3. The downstream outer edge of the flame holder was 18.6 inches in diameter and was located 41.8 inches from the pilot discharge. Thus an annular gap, 0.7 inches wide, existed between the downstream end of the flame holder and the combustion chamber wall. A slightly conical 38.6-inch-long fuel-air-mixture control sleeve, which enclosed 49 percent of the surface open area of the can, was attached to the flame holder. The upstream outer edge of the sleeve was 14.5 inches in diameter. The sleeve divided the flow area into inner and outer zones, each zone having its own fuel-injection system. Support struts were provided about midway along the control sleeve. The combustion chamber was 86 inches in length, measured axially from the base of the diffuser centerbody to the entrance of the exhaust nozzle.

Fuel-system details are shown in figure 3. Dual supply pipes fed and supported each of the three inner manifolds. Inner-zone manifolds and supply pipes were covered with a metal jacket to insulate them from the high-temperature inlet air. Each inner manifold had six spray bars which provided normal fuel injection from two opposed 0.021-inch-diameter holes. Each of the three outer manifolds was fed and supported by dual supply pipes and injected fuel in a downstream direction from five pairs of 0.028-inch-diameter holes. Inner- and outer-zone fuel was injected at distances of 16 and 13 inches, respectively, upstream of the pilot discharge.

Configuration 2. - Configuration 2 was the same as configuration 1 except that the flow restriction in the outer zone was increased by closing the 0.7-inch annular gap at the downstream end of the flame holder by

a flat plate (fig. 4). This plate was installed to shift the division of air flow between the inner and outer zones so that the inner-zone peak efficiency would be closer to a fuel-air ratio of 0.02.

Configuration 3. - Except for the inner-zone fuel-injection system and the combustion-chamber length, configuration 3 was identical to configuration 2. The fuel system was the same as that for configuration 2 except that the inner manifolds each had four spray bars and each bar provided normal fuel injection from two opposed 0.026-inch-diameter holes. The combustion-chamber length of configuration 3 was decreased to 56 inches to determine its effect on the can-type flame-holder performance.

Instrumentation

The locations of temperature and pressure instrumentation at the various stations are shown in figures 1 and 2. Engine-inlet total pressure and total temperature were measured in the surge tank upstream of the supersonic nozzle. Wall static pressure was measured near the engine subsonic-diffuser exit. A water-cooled rake, just upstream of the engine exhaust-nozzle inlet, provided a total-pressure survey. Air flows to the preheater and pilot burner were measured with A.S.M.E. type flat-plate orifices. Temperature of the pilot air was measured downstream of the pilot-air metering orifice. Fuel flows to both the combustion preheater and the engine were measured with calibrated rotameters. A periscope, used to determine engine blow-out, afforded visual observation of the combustion chamber from the exhaust nozzle; the line of sight was upstream along the engine axis.

PROCEDURE

Simulation of Flight Conditions

A free-jet Mach number of approximately 3.0 was obtained ahead of the engine by means of a convergent-divergent nozzle. By using the combustion-type preheater, the total temperature of the air entering the surge tank and pilot was raised to 1100° R to simulate the standard total temperature for a flight Mach number of 3.0 at altitudes above the tropopause.

The engine, by virtue of its inlet and exit geometry, operated supercritically for all fuel-air ratios (ref. 5). The combustor pressures are therefore somewhat lower for the simulated altitudes of this investigation than are obtainable with a better matching of the inlet and exit geometry. The performance of the three configurations invest-

igated is therefore presented both in terms of engine unit air flow and in terms of corresponding altitudes in the jet. For both the free-jet and direct-connect investigations, the total pressure in the surge tank was varied to provide a range of engine unit air flow. This range was from 4.09 to 6.85 pounds per second per square foot of combustion chamber cross-sectional area, corresponding to simulated altitudes of from 80,700 feet to 70,400 feet, respectively.

Operational Techniques

Supersonic flow was established in the free-jet nozzle at the inlet temperature of 1100° R. A throttling valve downstream of the engine exhaust nozzle (fig. 1) was then partially closed to raise the combustor pressure level and reduce the velocity at the combustor inlet. Next, the engine ignition system was activated, after which fuel was supplied to the inner-zone manifolds in the desired amount. Upon ignition of the fuel-air mixture, the throttling valve was opened and the engine exhaust nozzle was choked. Data were taken at constant unit air flow, and the engine inner-zone fuel flow was varied to cover the operable range of fuel-air ratio. Then, while fuel flow to the inner zone was held constant at the most efficient inner-zone fuel-air ratio, fuel was supplied to the outer zone to determine the performance at richer fuel-air ratios.

Symbols and Calculations

Symbols used in this report are listed in appendix A. Methods of calculation of engine-inlet air flow, engine fuel-air ratio, combustor efficiency, combustor-inlet Mach number, and specific fuel consumption are listed in appendix B.

RESULTS AND DISCUSSION

Configuration 1

The performance of configuration 1 is presented in figure 5(a) for unit air flows of 6.85, 5.42, and 4.09 pounds per second per square foot of combustion-chamber cross-sectional area. Performance was measured with inner-zone fuel injection only. A peak combustor efficiency of 0.86 was obtained at a fuel-air ratio of 0.013 (fig. 5(a)), leaner than the desired fuel-air ratio of 0.02, for a unit air flow of 6.85. At the low unit air flow of 4.09, the peak combustor efficiency occurred at a fuel-air ratio of 0.016 and was only 0.52. The combustor pressure ratio was about 0.95 for all burning conditions. The combustor-exit total pressure varied from 470 to 1090 pounds per square foot absolute. The combustor-inlet Mach number varied from 0.32 to 0.22.

Configuration 2

In order to shift the inner-zone peak-efficiency point of configuration 1 to a higher fuel-air ratio (around 0.02) it was necessary to pass a larger percentage of the total engine air flow through the inner zone. The increase in air flow through the inner zone was accomplished with configuration 2 by increasing the flow restriction in the outer zone.

The performance of configuration 2 is presented in figure 5(b) for approximately the same unit air flows as for configuration 1. For operation with only the inner-zone fuel system, a peak combustor efficiency of 0.90 occurred at a fuel-air ratio of 0.018 (unit air flows of 5.44 and 6.80). Thus, the objective of shifting the inner-zone peak-efficiency fuel-air ratio nearer to a fuel-air ratio of 0.02 was achieved and, in addition, the peak efficiency was increased by about 5 percentage points for the unit air flows of 6.80 and 5.44. For operation at a unit air flow of 4.10, the peak efficiency showed a marked increase from 0.52 to 0.87 with configuration 2. These improvements in efficiency, however, were gained at the expense of increased combustor pressure losses as shown by comparison of figures 5(a) and (b). Configuration 2 had a combustor pressure ratio of 0.89, whereas configuration 1 had a pressure ratio of 0.95. In a subsequent paragraph, the combined effects of efficiency and combustor pressure ratio on specific fuel consumption will be discussed.

When configuration 2 was operated with inner and outer fuel systems together, peak combustor efficiency occurred at a fuel-air ratio of about 0.04. The peak combustor efficiency was about 0.90 for both unit air flows investigated.

The effect of pressure over a wider range than that covered by these tests can be revealed by comparison with reference 3, where combustor-inlet pressures of 2230 to 2530 pounds per square foot were experienced. In reference 3, efficiencies of 0.9 or better were obtained at all fuel-air ratios. Configuration 2 had peak efficiencies of 0.88 to 0.91 at pressures from 600 to 1400 pounds per square foot for fuel-air ratios of about 0.018 and 0.04, but was 13 percentage points lower in the fuel-air-ratio range from 0.02 to 0.03. Hence, the effect of reducing pressure was to reduce the combustor efficiency at fuel-air ratios where the transition between inner-zone fuel injection and fuel injection in both zones occurs, but there was little effect on peak combustor efficiency. The combustor-inlet velocities reported in reference 3 were somewhat lower than for configuration 2, but it is felt that this effect was negligible.

Specific Fuel Consumption (Comparison with Other Combustor Types)

The range of a ram-jet powered missile is dependent upon both the combustor efficiency and the combustor pressure ratio. These parameters are combined in the parameter specific fuel consumption, which is an index of range potential. Accordingly, the specific fuel consumption was calculated for these data for purposes of comparison. A diffuser total-pressure recovery of 0.6 and a completely expanded exhaust nozzle having a velocity coefficient of 0.95 were assumed for this calculation. Variation of specific fuel consumption with net thrust per pound of engine air flow is shown in figure 6 for configurations 1, 2, and a typical circular V-gutter configuration (ref. 1, configuration 6) for a unit air flow of approximately 6.8. Lines of constant fuel-air ratio and a line indicating the ideal combustor performance (based on a combustor efficiency of 1.0 and the appropriate pressure loss of heat addition) are given for reference. Configuration 1 had a minimum specific fuel consumption of 2.08 at a fuel-air ratio of 0.013. Configuration 2 had a slightly lower minimum specific fuel consumption of 2.05 for the lean fuel-air ratio range. Thus, the higher flame-holder pressure loss largely nullified the advantage of higher combustor efficiency which configuration 2 had over configuration 1. The minimum specific fuel consumption for the typical circular V-gutter configuration was 2.15, which occurred at a fuel-air ratio of 0.018. For the lean range of fuel-air ratio, configuration 2 and configuration 6 of reference 1 had nearly the same specific fuel consumption (within 4 percent). At fuel-air ratios above 0.042, the can combustor was slightly inferior to configuration 6 of reference 1.

Effect of Shortening Combustion Chamber

Short combustion chambers are generally desirable from the standpoint of weight and external drag considerations. To investigate the effect of shortening the can-type combustion chamber, configuration 3 was tested. This configuration was the same as configuration 2 except that: (a) the combustion chamber was shortened from 86 to 56 inches, and (b) the inner-zone fuel-injection system was modified slightly as discussed in APPARATUS. The fuel-system design change was felt to have a negligible effect upon performance.

Data for the performance of configuration 3 were obtained by the direct-connect mode of investigation and are presented in figure 7 together with the direct-connect performance data of configuration 2. All the data presented in this curve were obtained at a unit air flow of approximately 6.8. The peak value of efficiency of 0.77, with only inner-zone fuel injection (fig. 7), occurred at a fuel-air ratio of 0.02 for configuration 3. This was 14 percentage points lower than the efficiency of configuration 2 for the same fuel-air ratio. At this same

fuel-air ratio, the combustor efficiency of the typical V-gutter configuration of figure 6 was lowered 8 percentage points by shortening the combustion chamber in a similar manner (ref. 1). Thus, it appears that the can-type flame-holder combustor efficiency was more sensitive to combustion-chamber length than the efficiency of the typical V-gutter configuration.

In the range of fuel-air ratio up to 0.05, the efficiency of configuration 2 was markedly superior to that of the shorter configuration 3; for example, at a fuel-air ratio of 0.04, the efficiency of configuration 2 was 18 percentage points higher than the efficiency of configuration 3. Above a fuel-air ratio of 0.0525, however, the efficiencies were approximately equal, indicating that length had little effect at fuel-air ratios near stoichiometric. Combustor total-pressure ratios of configurations 2 and 3 were essentially equivalent (fig. 7).

Effect of Pilot-Burner Variables

As part of the investigation of the performance of configuration 2, a brief study of the effects of pilot variables on combustor efficiency and stability limits with only inner-zone fuel injection was undertaken. The effect of percent pilot air flow on combustor efficiency at a fuel-air ratio of about 0.015 and a unit air flow of about 6.9 is presented in figure 8. Over the range of pilot air flow investigated, combustor efficiency decreased slightly with increased percent pilot air flow. With 3 percent pilot air flow, the combustor efficiency decreased about 3 percent below its level with no pilot air flow. Thus, although the trend is slight, it appears that combustor efficiency was adversely affected by increasing the pilot air flow.

The effects of pilot air flow and pilot fuel flow upon inner-zone stability limits are shown in figure 9, where lean and rich blow-out limits are plotted against pilot fuel flow for three pilot air flows. The regions of stable combustion broadened with increasing percent pilot air flow. Increasing pilot fuel flow decreased the rich limit of stable combustion in each case. Fairly wide stability limits can be achieved (0.001 to 0.028) by using 1 percent pilot air and a pilot fuel flow of 1 percent of over-all stoichiometric. This mode of pilot operation would have only negligible effect on combustor efficiency as shown by figure 8.

SUMMARY OF RESULTS

An investigation of three configurations of can-type combustors employing a fuel-air-mixture control sleeve and a dual (inner and outer zone) fuel system in a 20-inch-diameter ram-jet combustor was conducted in a facility simulating flight at Mach number 3.0 and altitudes from about 70,000 to 80,000 feet. The following results were obtained:

1. One configuration had peak combustor efficiencies of about 0.90 at fuel-air ratios of 0.018 and 0.04. When compared with the results of a previous investigation of a similar can-type combustor at higher combustor pressures, it was found that a reduction in combustor pressure from over 2000 to less than 1000 pounds per square foot introduced a reduction in the combustor efficiency at fuel-air ratios in the transition region between inner-zone fuel injection and fuel injection in both zones but had little effect on peak efficiency.

2. To enable a comparison with other combustors, specific fuel consumption was calculated. The comparison showed that the performance of the can-type combustor differed only slightly from the performance of a typical circular V-gutter configuration. At a fuel-air ratio of 0.018, the can-type combustor had about 4 percent lower specific fuel consumption, but was slightly inferior at fuel-air ratios above 0.042.

3. It was found that reducing the combustion-chamber length from 86 to 56 inches caused a reduction in combustor efficiency for the can-type flame holder of 14 percentage points at a fuel-air ratio of 0.02 and of 18 percentage points at a fuel-air ratio of 0.04. Above a fuel-air ratio of 0.0525, however, the efficiencies were not affected by the change in length.

4. The range of fuel-air ratio for which stable inner-zone burning was possible was found to be increased by burning fuel in the small center pilot, but increases in pilot air flow over 1 percent of total air flow caused a small reduction in combustor efficiency. When the pilot was operated with 1 percent air flow and a fuel flow of 1 percent of overall stoichiometric, fairly wide stability limits were provided with a negligible loss of combustor efficiency.

Lewis Flight Propulsion Laboratory
National Advisory Committee for Aeronautics
Cleveland, Ohio, April 15,1954

APPENDIX A

SYMBOLS

The following symbols are used in this report:

A	area, sq ft
a	local speed of sound, ft/sec
B	fraction of supersonic jet flow entering engine inlet
C_d	discharge coefficient of exhaust nozzle
C_v	velocity coefficient of exhaust nozzle
F_n	net thrust, lb
f/a	engine fuel-air ratio
$(f/a)'$	ideal fuel-air ratio
$(f/a)_p$	fuel-air ratio of preheater
$(f/a)_s$	stoichiometric fuel-air ratio
g	acceleration due to gravity, 32.2 ft/sec^2
M	Mach number
P	total pressure, lb/sq ft abs
p	static pressure, lb/sq ft abs
R	gas constant, ft-lb/(lb)($^\circ$R)
T	total temperature, $^\circ$R
t	static temperature, $^\circ$R
sfc	specific fuel consumption, $\frac{\text{lb fuel/hr}}{\text{lb net thrust}}$
V	velocity, ft/sec
W	engine air flow, $(W_i + W_p)$, lb/sec
$W_{f,e}$	fuel flow to engine (including pilot fuel flow), lb/sec

$W_{f,p}$ fuel flow to preheater, lb/sec

W_i engine inlet air flow (measured at exhaust nozzle when $W_P = 0$), lb/sec

W_P pilot air flow, lb/sec

W_p air flow to preheater, lb/sec

W_u unburned air flow entering engine, lb/sec

γ ratio of specific heats

η combustor efficiency

ρ density, lb/cu ft

Subscripts:

c cold (engine not burning and no pilot air flow)

h hot (engine burning)

0 free stream

2 subsonic diffuser exit

3 conditions at station 2 adjusted to combustion-chamber area

4 exhaust-nozzle inlet

5 exhaust-nozzle minimum area

6 station downstream of exhaust-nozzle exit

APPENDIX B

METHODS OF CALCULATION

Engine-inlet air flow. - The engine exhaust nozzle served as a convenient metering orifice for determining the rate of flow of air through the engine inlet for nonburning conditions (with no pilot air flow and the assumption that leakage through the engine flanges was negligible). The engine-inlet air flow was calculated from the mass-flow equation

$$W_i = \rho_{5,c} C_{d,c} A_5 V_{5,c} \tag{1}$$

The exhaust nozzle was choked at its minimum area ($M_5 = 1$); thus, W_i was expressed as

$$W_i = \frac{P_{5,c} C_{d,c} A_5 \sqrt{\gamma g}}{\left(\frac{\gamma + 1}{2}\right)^{\frac{\gamma+1}{2(\gamma-1)}} \sqrt{RT_{5,c}}} \tag{2}$$

where $P_{5,c}$ and $T_{5,c}$ were assumed equal to $P_{4,c}$ and T_0, respectively. The exhaust-nozzle discharge coefficient $C_{d,c}$ was assumed to be 0.985. Pilot air flow W_P was metered with an A.S.M.E. flat-plate orifice. Total engine air flow W was then $W_i + W_P$.

Engine fuel-air ratio. - The engine fuel-air ratio was defined as the ratio of the engine fuel flow to the unburned air flowing into the combustor. Leaving the preheater was a gas which had a fuel-air ratio of

$$(f/a)_p = \frac{W_{f,p}}{W_p} \tag{3}$$

where W_p is the preheater air flow measured by an A.S.M.E. flat-plate orifice. It was found that the preheater combustion efficiency was nearly 100 percent. The ratio B of the engine-inlet air flow to the supersonic nozzle flow was constant because the engine-inlet diffuser operated supercritically at all times. The unburned air passing into the engine combustion chamber was then

$$W_u = \left[(W_p - W_P)\, B + W_P\right] \left[1 - \frac{(f/a)_p}{(f/a)_s}\right] \tag{4}$$

This is different from W_i which includes preheater products of combustion. The engine fuel-air ratio was then

$$f/a = \frac{W_{f,e}}{\left[BW_p + W_p(1-B)\right]\left[1 - \frac{(f/a)_p}{(f/a)_s}\right]} \tag{5}$$

Because it was more convenient to measure the engine-inlet air flow than BW_p, use was made of the following relation:

$$W = W_i + W_p = BW_p\left[1 + (f/a)_p\right] + W_p(1-B) \tag{6}$$

Rearranging terms gives

$$BW_p = \frac{W - W_p(1-B)}{\left[1 + (f/a)_p\right]} \tag{7}$$

Substitution of equation (7) in equation (5) gives

$$f/a = \frac{W_{f,e}/W}{1 + \frac{W_p}{W}(1-B)(f/a)_p} \times \frac{1 + (f/a)_p}{1 - \frac{(f/a)_p}{(f/a)_s}} \tag{8}$$

The term $\frac{W_p}{W}(1-B)(f/a)_p$ was inconsequential in magnitude and was assumed to be zero in all calculations.

Combustor efficiency. - The combustor efficiency η was defined as

$$\eta = \frac{(f/a)'}{(f/a)} \tag{9}$$

where f/a is given by equation (8) and $(f/a)'$ is the ideal fuel-air ratio which would have produced the same combustor-exit total pressure P_4 as was measured for the burning conditions under consideration. Thus, the efficiency was related only to combustor-exit total pressure, obviating the direct measurement of the high combustion-chamber temperatures.

The determination of $(f/a)'$ was implemented in the following way: The engine air flow at a given simulated altitude was the same for the nonburning and burning conditions and could be expressed as

$$W = \rho_{5,c} C_{d,c} A_5 V_{5,c} = \frac{\rho_{5,h} C_{d,h} A_5 V_{5,h}}{1 + \frac{W_{f,e}}{W}} \tag{10}$$

By using the equation of state, converting static pressure and temperature to total values, converting velocity to Mach number, and rearranging equations (10), the following expressions may be written:

$$P_{5,h} = \frac{W\left(1 + \frac{W_{f,e}}{W}\right)}{C_{d,h} A_5 M_{5,h}} \sqrt{\frac{R_h T_{5,h}}{\gamma_h g}} \left(1 + \frac{\gamma_h - 1}{2} M_{5,h}^2\right)^{\frac{\gamma_h + 1}{2(\gamma_h - 1)}} \tag{11}$$

and

$$P_{5,c} = \frac{W}{C_{d,c} A_5 M_{5,c}} \sqrt{\frac{R_c T_{5,c}}{\gamma_c g}} \left(1 + \frac{\gamma_c - 1}{2} M_{5,c}^2\right)^{\frac{\gamma_c + 1}{2(\gamma_c - 1)}} \tag{12}$$

Dividing equation (11) by equation (12), and assuming that

$$P_{5,c} = P_{4,c} \tag{13}$$

$$P_{5,h} = P_{4,h} \tag{14}$$

$$T_{5,c} = T_{4,c} = T_0 \tag{15}$$

$$T_{5,h} = T_{4,h} \tag{16}$$

$$C_{d,h} = C_{d,c} \tag{17}$$

and noting that

$$M_{5,c} = M_{5,h} = 1 \tag{18}$$

yields the following equation:

$$\frac{P_{4,h}}{P_{4,c}} = \sqrt{\frac{T_{4,h}}{T_0}}\left(1 + \frac{W_{f,e}}{W}\right)\sqrt{\frac{\left[\left(\frac{\gamma+1}{2}\right)^{\frac{\gamma+1}{\gamma-1}}\left(\frac{R}{\gamma}\right)\right]_h}{\left[\left(\frac{\gamma+1}{2}\right)^{\frac{\gamma+1}{\gamma-1}}\left(\frac{R}{\gamma}\right)\right]_c}}$$

The pressure ratio $P_{4,h}/P_{4,c}$ was then evaluated for various ideal fuel-air ratios by using theoretical combustion charts, which included the effects of dissociation, to find $T_{4,h}$. These data were then plotted as $(f/a)'$ against $P_{4,h}/P_{4,c}$. By referring to this plot, the ideal fuel-air ratio $(f/a)'$ could be obtained for each value of $P_{4,h}/P_{4,c}$ measured in the engine combustion chamber.

The combustor efficiency as defined herein is not a chemical combustion efficiency such as a heat-balance or enthalpy-rise method would indicate. The combustor efficiency based on total-pressure measurement is more representative of over-all engine performance, because it indicates how effectively the fuel is being used to provide thrust potential rather than how completely the fuel is being burned.

Combustor-inlet Mach number. - The combustor-inlet Mach number was calculated by using the engine air flow W, the static pressure measured at station 2 p_2, the inlet total temperature T_0, and the maximum area of the combustion chamber (314.2 sq in.).

Specific fuel consumption. - The specific fuel consumption was calculated as the ratio of the engine fuel flow in pounds per hour to the net thrust. Thus

$$sfc = \frac{3600\left(W_{f,e}\right)}{F_n} \tag{20}$$

where F_n, the net thrust, is given by

$$F_n = \frac{W}{g} V_6 C_v (1+f/a) + A_6(p_6 - p_0) - \frac{W}{g} V_0 \tag{21}$$

By substituting equation (21) into equation (20) and rearranging, equation (20) can be expressed as

$$sfc = \frac{3600\ g \left(\frac{W_{f,e}}{W}\right)}{V_6 C_V (1 + f/a) + \frac{A_6}{W} g(p_6 - p_0) - V_0} \tag{22}$$

For this expression, $W_{f,e}/W$ was considered equivalent to f/a of equation (8). The exhaust gases were assumed to be completely expanded to atmospheric pressure; hence, the quantity $(A_6/W)g(p_6 - p_0)$ is zero. The value C_v was taken as 0.95.

The velocity V_6 was determined as follows:

$$V_6 = M_6 a_6 \tag{23}$$

$$V_6 = M_6 \sqrt{\gamma_6 g R_6 t_6} \tag{24}$$

$$V_6 = M_6 \sqrt{\frac{\gamma_6 g R_6 T_6}{1 + \frac{\gamma_6 - 1}{2} M_6^2}} \tag{25}$$

The value M_6 was found from the exhaust nozzle pressure ratio P_4/p_0, where

$$\frac{P_4}{p_0} = \frac{P_2}{p_0} \frac{P_4}{P_2} \frac{P_0}{p_0} \tag{26}$$

The value P_2/P_0 was assumed to be 0.60 (readily obtained in practice) for all the data; P_4/P_2 was the combustor total-pressure ratio. The ratio P_0/p_0 was 36.7 (a constant corresponding to flight at a Mach number of 3.0).

The temperature T_6 was determined from T_0, the combustor efficiency, and a curve of temperature rise against ideal fuel-air ratio. Thus, all the quantities in equation (25) are determined.

REFERENCES

1. Trout, Arthur M., and Wentworth, Carl B.: Free-Jet Altitude Investigation of a 20-Inch Ram-Jet Combustor with a Rich Inner Zone of Combustion for Improved Low-Temperature-Ratio Operation. NACA RM E52L26, 1953.

2. Henzel, James G., Jr., and Wentworth, Carl B.: Free-Jet Investigation of 20-Inch Ram-Jet Combustor Utilizing High-Heat-Release Pilot Burner. NACA RM E53H14, 1953.

3. Cervenka, A. J., Perchonok, Eugene, and Dangle, E. E.: Effect of Fuel Injector Location and Mixture Control on Performance of a 16-Inch-Ram-Jet Can-Type Combustor. NACA RM E53F15, 1953.

4. Wentworth, Carl B., Hurrell, Herbert G., and Nakanishi, Shigeo: Evaluation of Operating Characteristics of a Supersonic Free-Jet Facility for Full-Scale Ram-Jet Investigations. NACA RM E52I08, 1952.

5. Smolak, George R., and Wentworth, Carl B.: Altitude Performance of a 20-Inch-Diameter Ram-Jet Engine Investigated in a Free-Jet Facility at Mach Number 3.0. NACA RM E52K24, 1953.

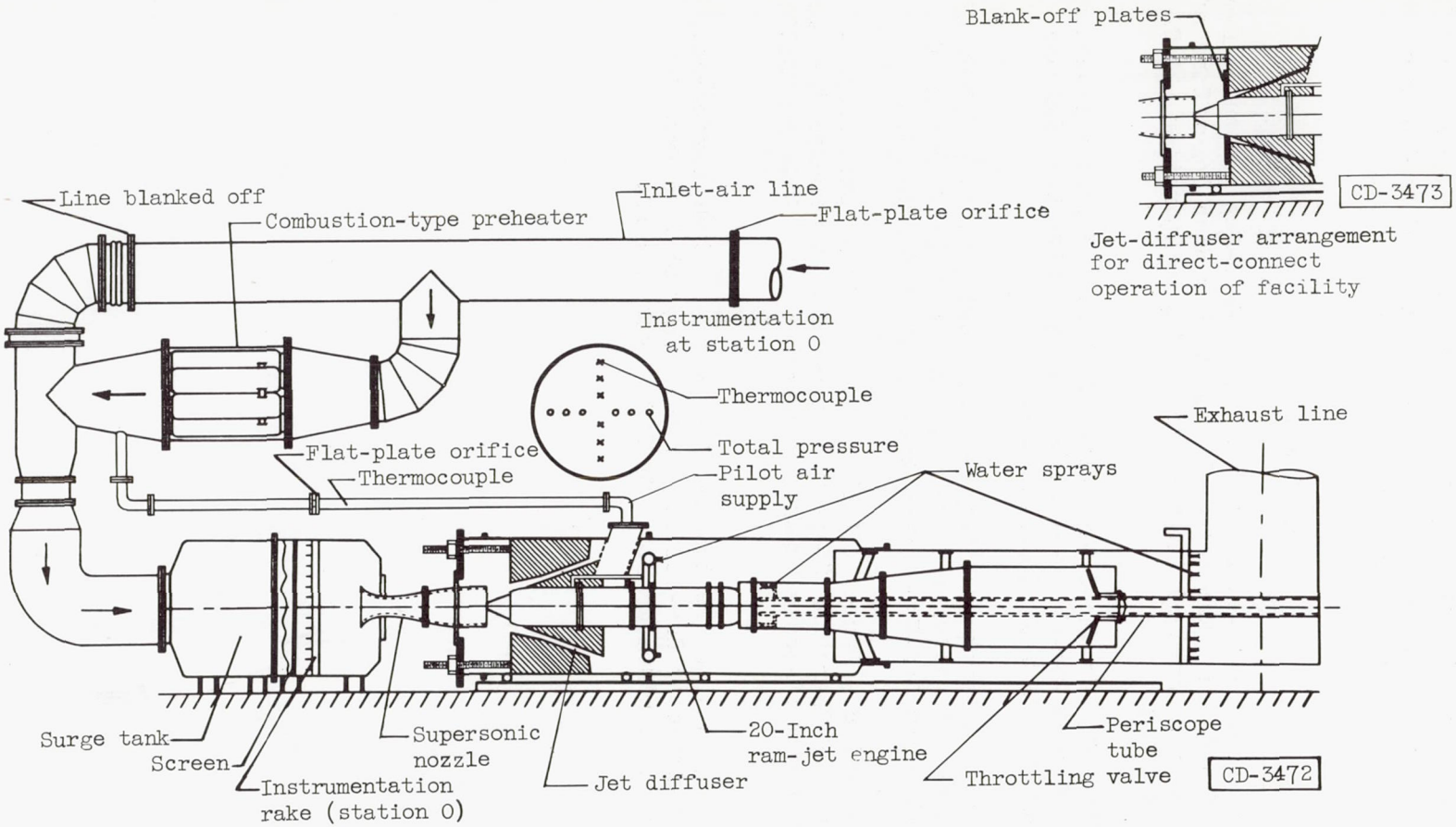

Figure 1. - Free-jet facility with 20-inch-diameter ram-jet engine installed.

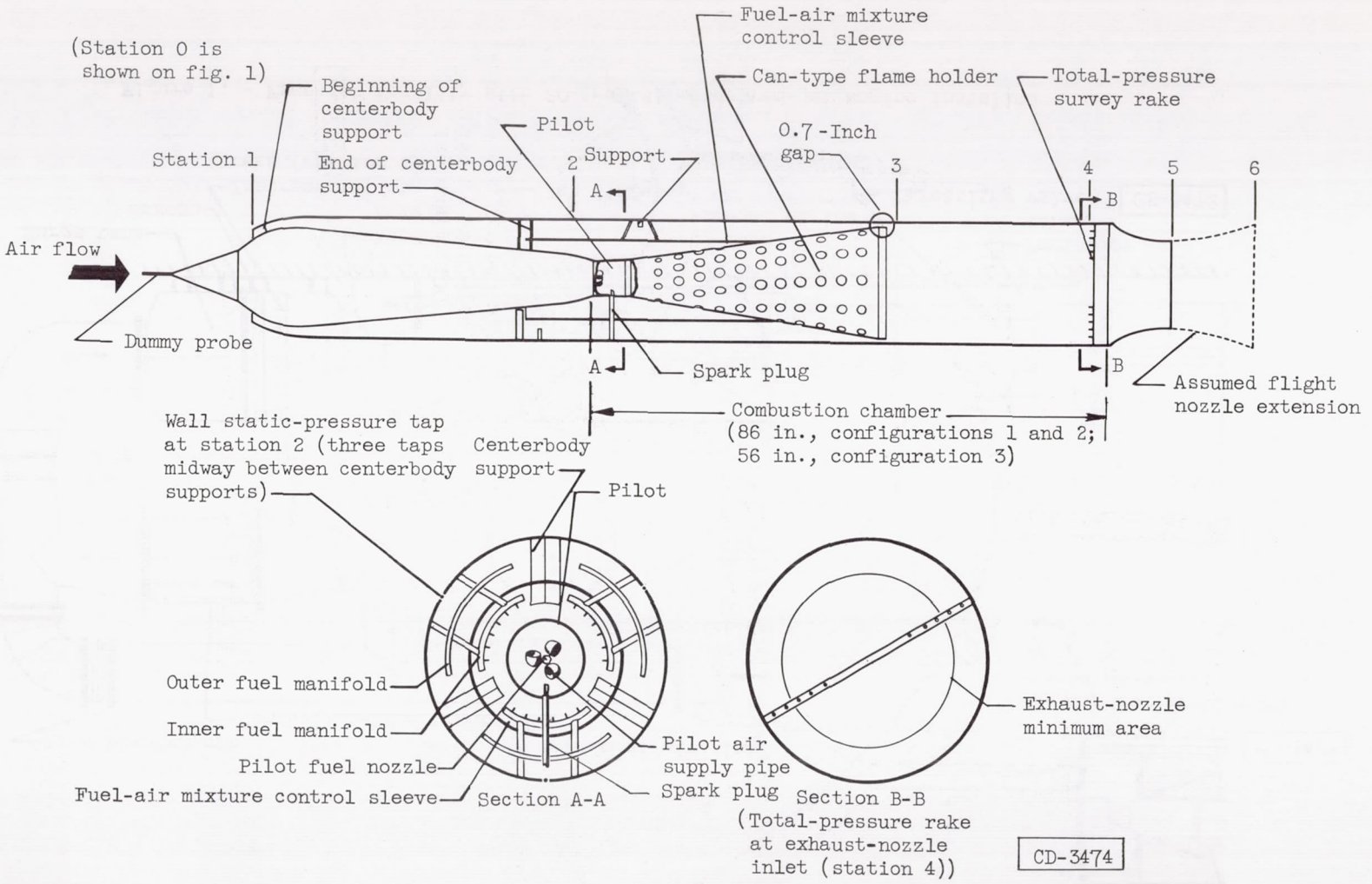

Figure 2. - 20-Inch-diameter ram-jet engine with can-type flame holder installed.

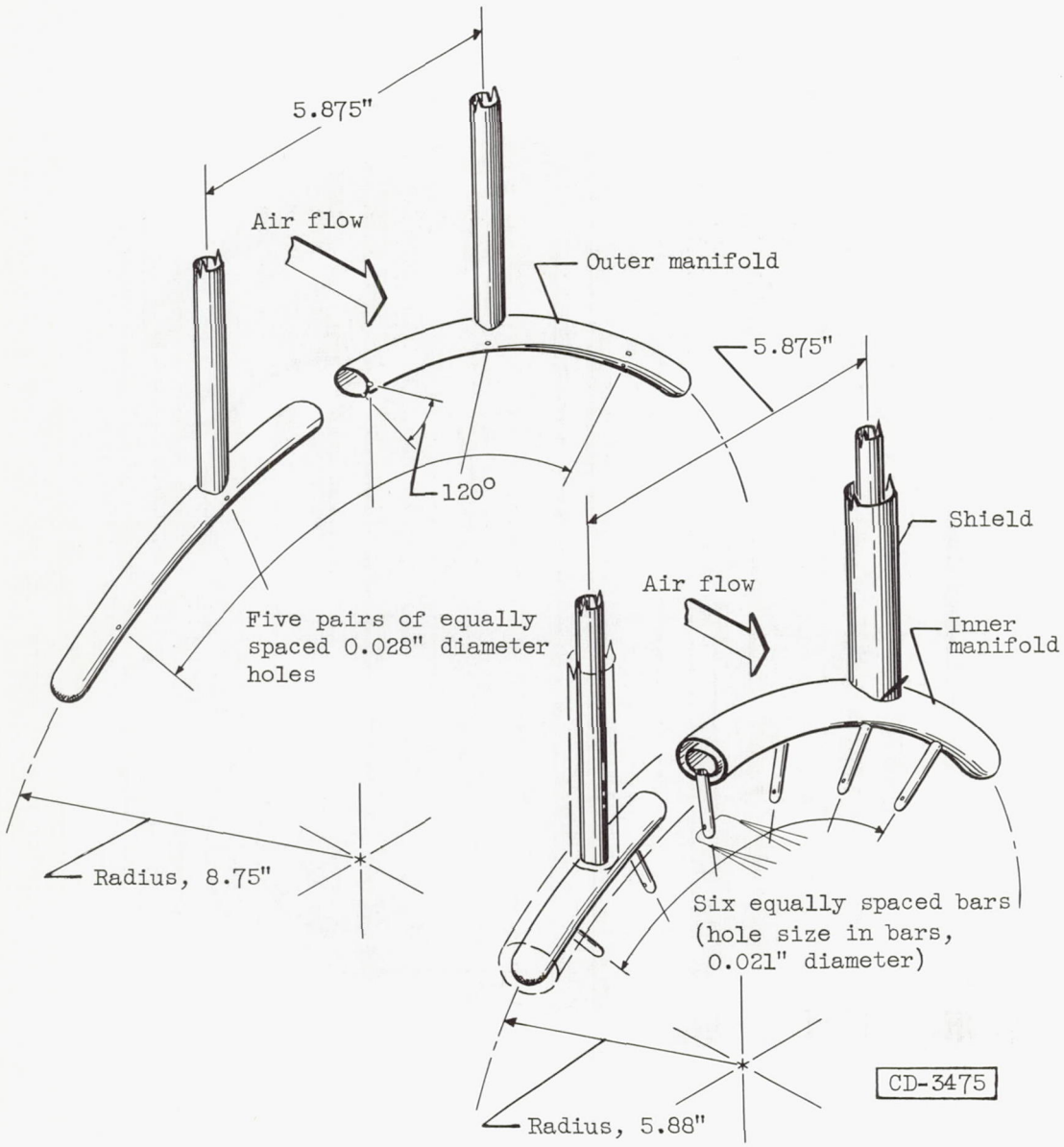

Figure 3. - Fuel-system details.

(a) Viewed looking upstream.

Figure 4. - Can-type flame holder with fuel-air mixture control sleeve attached (used for configurations 2 and 3).

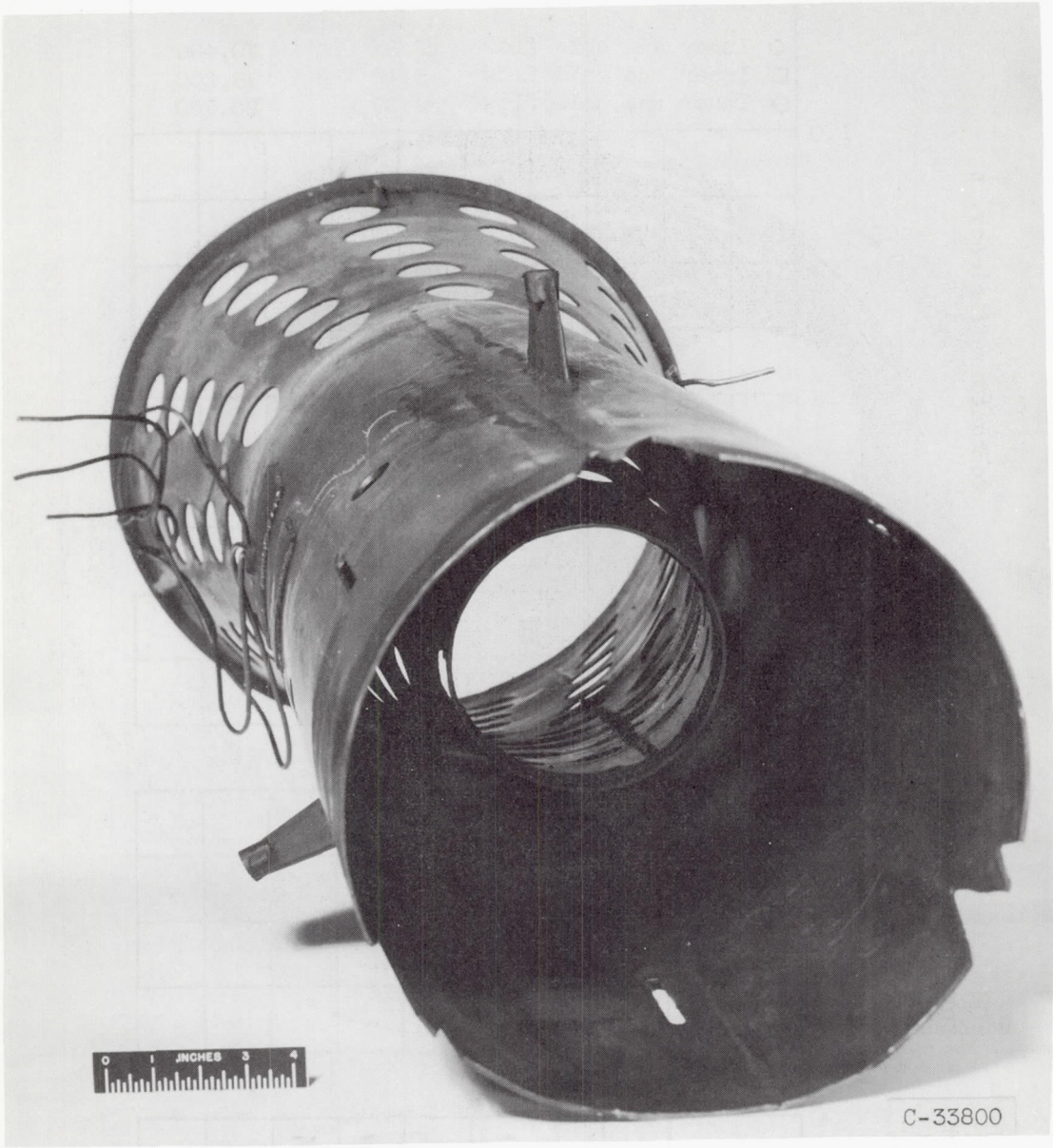

(b) Viewed looking downstream.

Figure 4. - Concluded. Can-type flame holder with fuel-air mixture control sleeve attached (used for configurations 2 and 3).

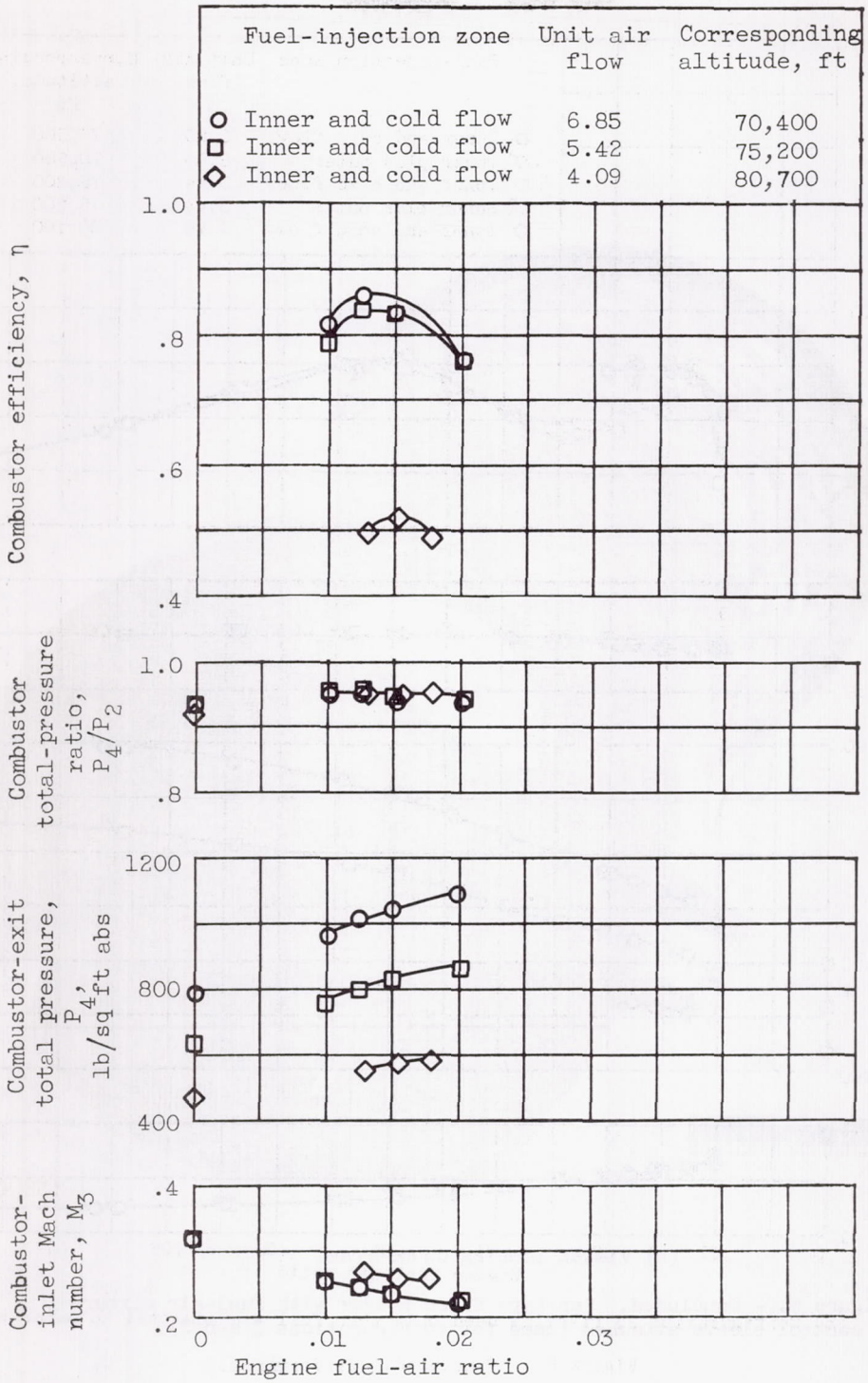

(a) Configuration 1; pilot not used.

Figure 5. - Performance.

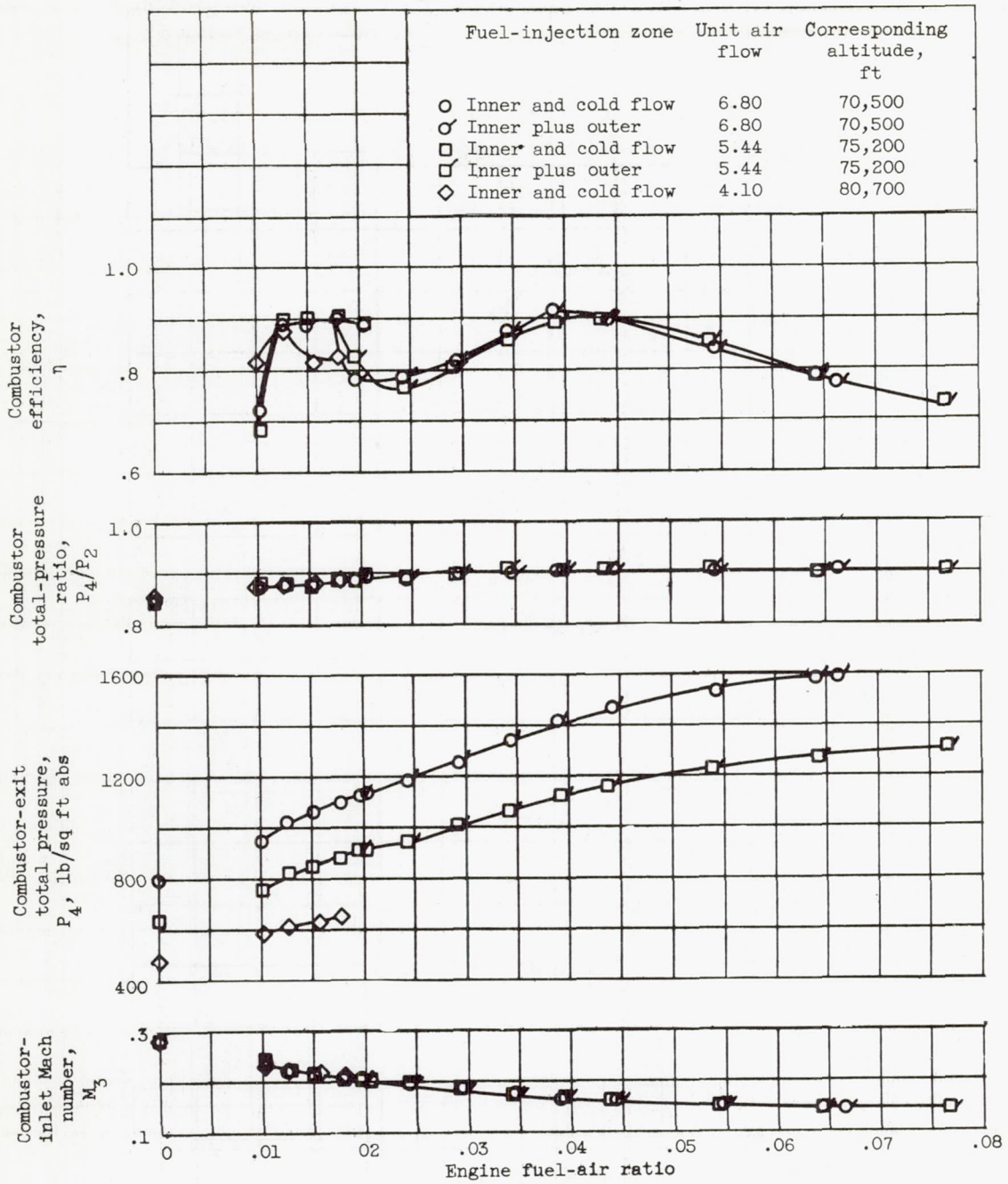

(b) Configuration 2; piloting used only when fuel was admitted to outer zone.

Figure 5. - Concluded. Performance.

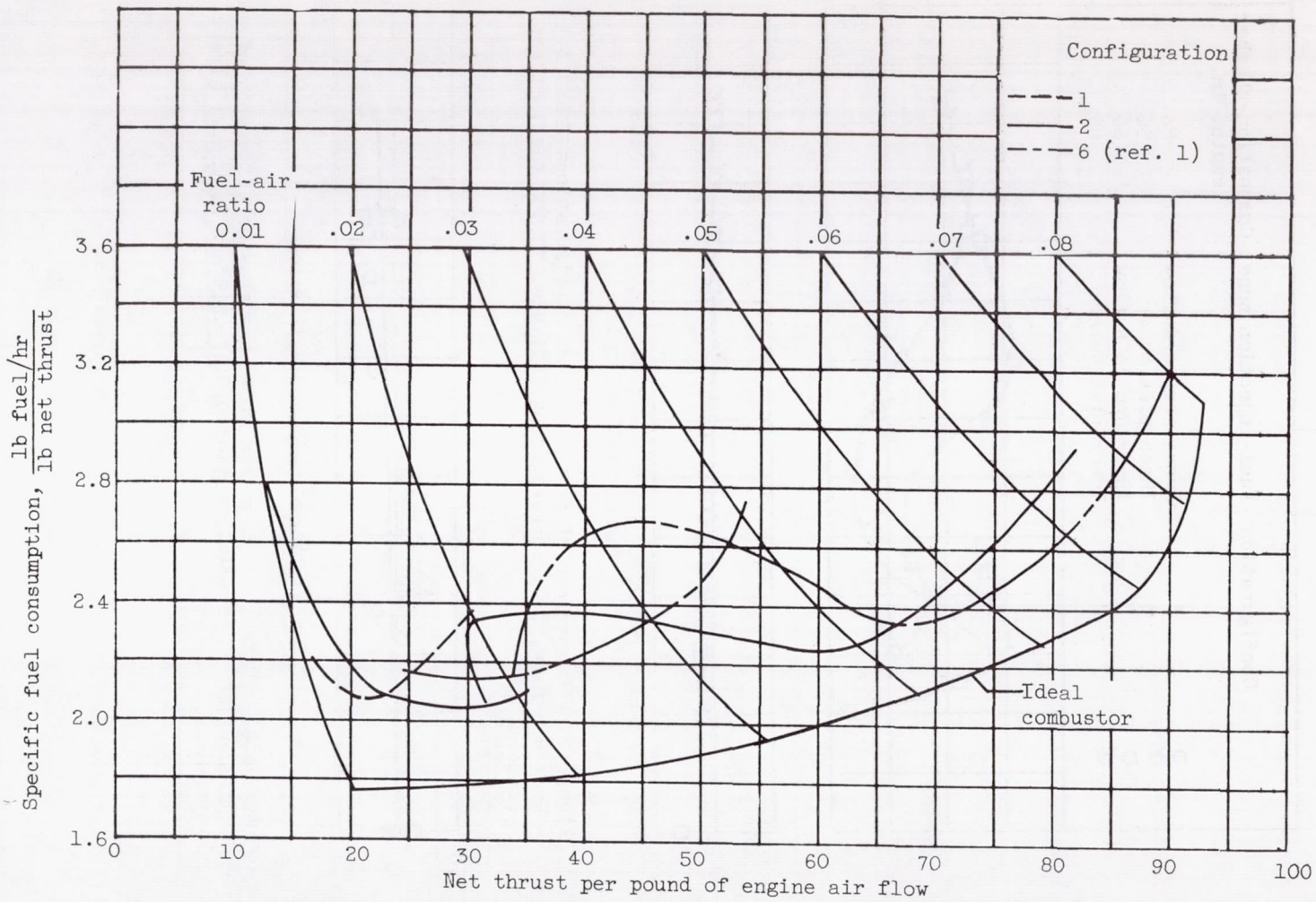

Figure 6. - Variation of specific fuel consumption with net thrust per pound of air flow. Diffuser total-pressure recovery, 0.6 (assumed); unit air flow, about 6.8 (simulated altitude, approximately 70,500 ft); combustion-chamber length, 86 inches.

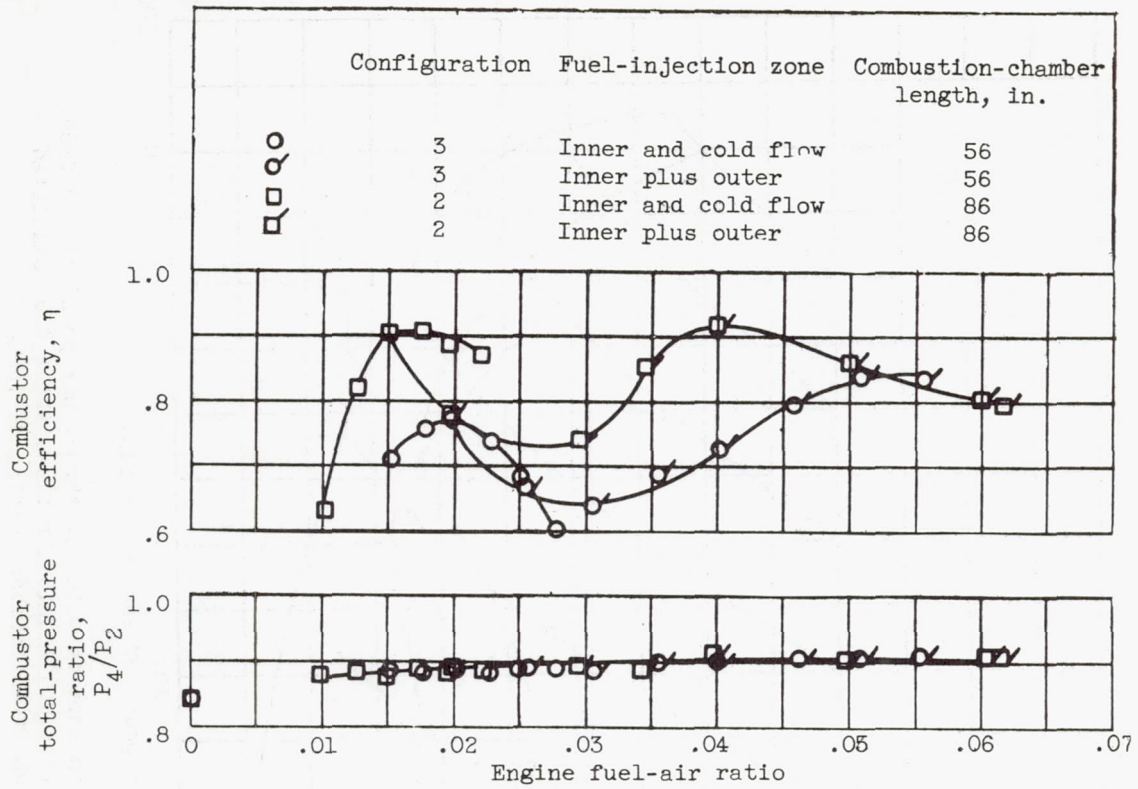

Figure 7. - Comparison of performance of configurations 2 and 3. Unit air flow, 6.8; corresponding altitude, 70,500 feet; direct connect.

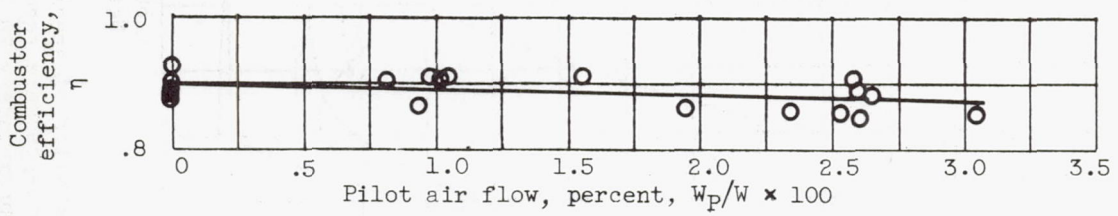

Figure 8. - Effect of pilot air flow on combustor efficiency of configuration 2. Fuel-air ratio; 0.015; unit air flow, 6.9; direct connect.

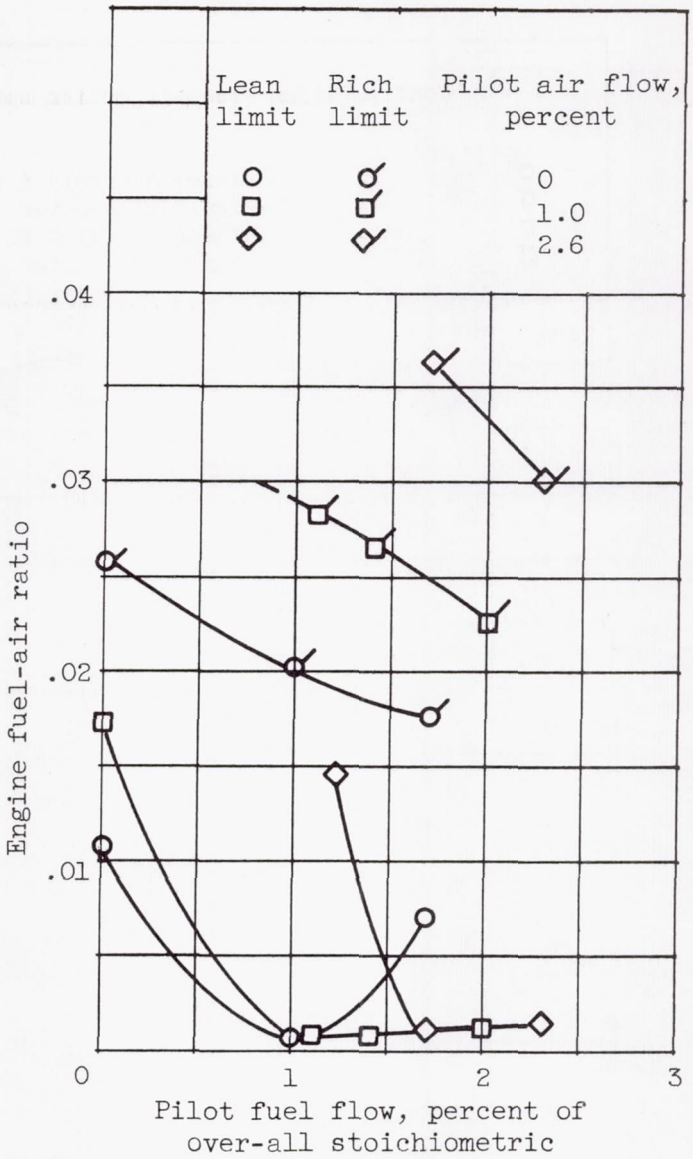

Figure 9. - Inner-zone stability limits for various pilot air flows and fuel flows. Configuration 2; unit air flow, 6.8.